

High-Field EPR Characterization of Manganese Reconstituted Superoxide Dismutase from *Rhodobacter capsulatus*

Sun Un,^{*,†} Pierre Dorlet,[†] Guillaume Voyard,[†]
Leandro C. Tabares,[‡] and Néstor Cortez[‡]

Section de Bioénergétique, CNRS URA 2096
CEA-Saclay, F-91191 Gif-sur-Yvette, France
Instituto de Biología Molecular y Celular de
Rosario (IBR), Universidad Nacional de
Rosario and CONICET, Suipacha 531
S20002LRK Rosario, Argentina

Received May 23, 2001

Metal specificity is an intriguing aspect of manganese- and iron-containing superoxide dismutases (SOD). Although there is a high degree of structural homology among these enzymes,¹ activity is highly metal-specific with virtually complete loss of activity when the non-native metal is bound.² Electron paramagnetic resonance (EPR) can be used to probe directly the protein–metal interactions that are at the heart of this specificity. However, a detailed quantitative understanding of the EPR spectra of the manganese(II) centers in these proteins is lacking.³ It is known that Mn(II) EPR spectra are sensitive to mutagenesis and effects of inhibitor binding.³ The size of the magnetic interactions which characterize these centers are not known with any certainty. We have used high-field EPR (HFEPR) to address this problem.

The low-temperature 285 GHz HFEPR of manganese-reconstituted SOD from *Rhodobacter capsulatus*⁴ and native MnSOD from *Escherichia coli*⁵ (Figure 1) exhibited similar

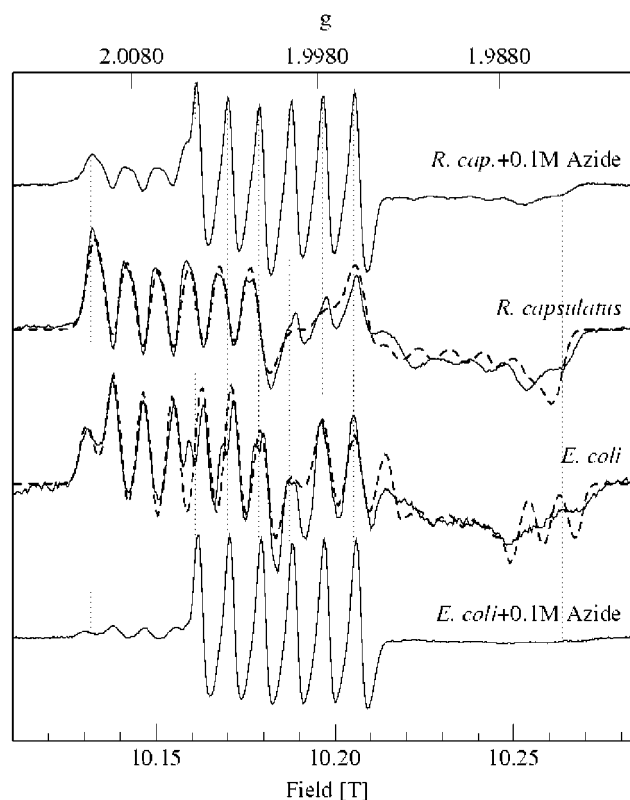


Figure 1. The 285 GHz EPR spectrum of the 0.1 mM manganese SOD in 10 mM Tris buffer at pH 8.2 from *R. capsulatus* (upper) and *E. coli* (lower) in the absence and presence of 0.1 M azide. Best-fit simulations are shown as dashed lines. Magnetic parameters are given in Table 1. Spectra were obtained at 25 K with 20 G modulation under nonsaturating conditions.

resonances centered near the free electron g -value at a value of 2.001 (Figure 1). This indicated that the dominant magnetic interaction at 10 T was the Zeeman interaction with the resonances corresponding to the $m_s = -1/2 \rightarrow 1/2$ transition of the $S = 5/2$ Mn(II) ions. The overall width of both resonances increased from 0.135 to 0.170 T when the microwave frequency was decreased from 285 to 190 GHz (data not shown). Therefore, the major contribution to the spectral width was neither g -anisotropy nor hyperfine interactions, but rather nonnegligible zero-field interaction, which has an inverse field-dependence.⁶

To compare quantitatively the two MnSOD spectra, simulations (Table 1 and Figure 1) were carried out using the third-order perturbation approximation⁷ to the $S = 5/2$ spin Hamiltonian⁸

$$H = g_{\text{iso}}\beta\mathbf{B}\cdot\mathbf{S} + A_{\text{iso}}\mathbf{I}\cdot\mathbf{S} + \frac{D}{3}[3S_z^2 - S(S+1)] + \frac{E}{2}(S_+^2 + S_-^2)$$

The terms describe the isotropic electronic Zeeman, nuclear hyperfine and zero-field interactions, respectively. The simulations and experimental spectra agreed nearly exactly for the low-field portion with greater differences at higher fields.⁹

(6) (a) Meirovitch, E.; Luz, Z.; Kalb (Gilboa), A. J. *J. Am. Chem. Soc.* **1974**, *27*, 7538–7542. (b) Meirovitch, E.; Luz, Z.; Kalb (Gilboa), A. J. *J. Am. Chem. Soc.* **1974**, *27*, 7542–7546.

(7) Markham, G. D.; Rao, B. D. N.; Reed, G. H. *J. Magn. Reson.* **1979**, *33*, 592–602.

(8) Simulation methods were similar to those described in: Polcar, C.; Knüpling, M.; Frapart, Y.-M.; Un, S. *J. Phys. Chem. B* **1998**, *102*, 10391–10398.

(9) The use of anisotropic g and hyperfine tensors did not change the quality of the simulations nor did the inclusion of nuclear quadrupole tensor terms.

[†] Section de Bioénergétique, CEA-Saclay, France.

[‡] IBR, Universidad Nacional de Rosario, Argentina.

(1) (a) Parker, M. W.; Blake, C. C. F. *J. Mol. Biol.* **1988**, *199*, 649–661. (b) Stoddard, B. L.; Howell, P. L.; Ringe, D.; Petsko, G. A. *Biochemistry* **1990**, *29*, 8885–8893. (c) Stoddard, B. L.; Ringe, D.; Petsko, G. A. *Protein Eng.* **1990**, *4*, 113–119. (d) Ludwig, M. L.; Metzger, A. L.; Patridge, K. A.; Stallings, W. C. *J. Mol. Biol.* **1991**, *219*, 335–358. (e) Borgstahl, G. E. O.; Parge, H. E.; Hickey, M. J.; Beyer, W. F.; Hallewell, R. A.; Tainer, J. A. *Cell* **1992**, *71*, 107–118. (f) Wagner, U. G.; Patridge, K. A.; Ludwig, M. L.; Stallings, W. C.; Werber, M. M.; Oefner, F. F.; Sussman, J. L. *Protein Sci.* **1993**, *2*, 814–825. (g) Edwards, R. A.; Baker, H. M.; Jameson, G. B.; Whittaker, M. M.; Whittaker, J. W.; Baker, E. N. *J. Biol. Inorg. Chem.* **1998**, *3*, 161–171. (h) Lah, M. S.; Dixon, M. M.; Patridge, K. A.; Stallings, W. C.; Fee, J. A.; Ludwig, M. L. *Biochemistry* **1995**, *34*, 1646–1660. (i) Cooper, J. B.; McIntyre, K.; Badasso, M. O.; Wood, S. P.; Zhang, Y.; Garbe, T. R.; Young, D. *J. Mol. Biol.* **1995**, *246*, 531–544. (j) Schmidt, M.; Meier, B.; Parak, F. *J. Biol. Inorg. Chem.* **1996**, *1*, 532–541. (k) Lim, J.-H.; Yu, Y. G.; Han, Y. S.; Cho, S.; Ahn, B.-Y.; Kim, S.-H.; Cho, Y. *J. Mol. Biol.* **1997**, *270*, 259–274. (l) Ursby, T.; Adinolfi, B. S.; Al-Karadaghi, S.; De Vendittis, E.; Bocchini, V. *J. Mol. Biol.* **1999**, *286*, 189–205. (m) Knapp, S.; Kardinahl, S.; Hellgren, N.; Tibbelin, G.; Schafer, G.; Ladenstein, R. *J. Mol. Biol.* **1999**, *285*, 689–702. (n) Sugio, S.; Hiraoka, B. Y.; Yamakura, F. *J. Biol. Chem.* **2000**, *267*, 3487–3495.

(2) Ose, D. E.; Fridovich, I. *J. Biol. Chem.* **1976**, *251*, 1217–1218. Hiraoka, B. Y.; Yamakura, F.; Sugio, S.; Nakayama, K. *Biochem. J.* **2000**, *345*, 345–350.

(3) (a) Schwartz, A. L.; Yakilmaz, E.; Vance, C. K.; Vathyam, S.; Koder, R. L.; Mill, A.-F. *J. Inorg. Biochem.* **2000**, *80*, 247–256. (b) Whittaker, M. M.; Whittaker, J. W. *Biochemistry* **1997**, *36*, 8923–8931. (c) Whittaker, M. M.; Whittaker, J. W. *J. Am. Chem. Soc.* **1991**, *113*, 5528–5540. (d) Fee, J. A.; Shapiro, E. R.; Moss, T. H. *J. Biol. Chem.* **1976**, *251*, 6157–6159.

(4) Cortez, N.; Carrillo, N.; Pasternak, C.; Balzer, A.; Klug, G. *J. Bacteriol.* **1998**, *180*, 5413–5420. *Rhodobacter* SOD coding region was amplified by PCR using the pA22 plasmid. A *Nco*I site was generated at the N terminus permitting cloning into an *E. coli* pET28 overexpression vector after *Nco*I/*Sac*I digestion. Isolated inclusion bodies from sonicated *E. coli* transformants were solubilized in 8 M urea. The denatured protein was refolded by dialysis against 1 mM MnSO₄ and further purified using ionic-exchange chromatography (Pharmacia Akta System, HiPrep 16/10 DEAE and MonoQ HR 5/5 columns). The active SOD component was collected and checked for purity by denaturing polyacrylamide gel electrophoresis.

(5) *E. coli* MnSOD purchased from Sigma-Aldrich was washed several times with 0.1 mM EDTA in 10 mM pH 8.2 Tris buffer to remove any adventitious manganese ions.

Table 1. Magnetic Parameters for the Mn(II) Centers in *R. capsulatus* and *E. coli* Superoxide Dismutases Obtained from Simulations (*D*, *E*, and A_{iso} Are in Units of 10^{-4} cm^{-1})¹⁰

	g_{iso}	<i>D</i>	<i>E</i>	A_{iso}
<i>R. capsulatus</i>	2.0009	3480	90	80
<i>E. coli</i>	2.0010	3440	295	77
<i>R. capsulatus</i> + 0.1 M azide ^a	2.0009	720	193	81
<i>E. coli</i> + 0.1 M azide ^a	2.0010	462	91	82

^a The *D* and *E* values were sensitive to the choice of inhomogeneous line-widths. Change in inhomogeneous line-width from 15 to 19 G resulted in a decrease in the *D* value of $20 \times 10^{-4} \text{ cm}^{-1}$. The reported values are those having the smallest root-mean-squared difference between experiment and simulation.

The biggest difference between the Mn centers in the two proteins was the zero-field *E* parameter. The four times greater *E. coli* *E* value was directly responsible for the differences in the lowest-field hyperfine features in the two spectra. As suggested by the amino acid sequence⁴ and the high degree of structural homology among the SODs for which the structure is known,¹ it is likely that the *R. capsulatus* SOD manganese centers have the same ligands as those in the *E. coli* protein and a similar trigonal bipyramidal geometry. If one assumes that the *z*-axis of the zero-field interaction is approximately along the Mn–OH (or solvent) direction,¹ the smaller *R. capsulatus* *E* values imply that the ligand–metal interactions in the equatorial plane are relatively more symmetric than in the *E. coli* protein.¹¹ The larger *R. capsulatus* *D* value indicates that the axial ligand interactions are also different.¹¹ Consistent with theoretical expectations,¹² the Mn(II) zero-field values are almost an order of magnitude smaller than those of the Mn(III) centers, reflecting the spherical nature of the five unpaired spins of the former.¹³ The hyperfine values are also clearly smaller than the Mn(III) value of $94.4 \times 10^{-4} \text{ cm}^{-1}$.¹³

Azide is known to bind to the SODs, converting the trigonal bipyramidal geometry of the center to an octahedral one.^{1h,14} Upon addition of 0.1 M azide, six sharp (35 G peak-to-peak) slightly asymmetric lines appeared in both *E. coli* and *R. capsulatus* HFEP spectra. In each case, the six lines were superimposed on a broader resonance which corresponded exactly to the respective spectrum of the native protein. The integrated intensity of the six-line spectra was no more than 25% that of the corresponding broad component. Free Mn(II) ions in aqueous buffer exhibited similar narrow six-line spectra. However, such spectra were quite different from those of azide-treated SOD samples, and hence, the possibility that azide addition resulted in the release of Mn ions could be excluded (see Supporting Information). We assigned the six-line spectrum to azide-bound Mn(II) centers. The narrowness of the signals compared to the width observed for those of the native protein is likely due to the fact that Mn(II) ions are hexa-coordinated.^{1h,3b,c} The 285 GHz spectra of the two azide-complexed proteins were virtually superimposable. 190 GHz spectra (Figure 2) were obtained to better estimate the zero-field parameters. Except for the resonant-field, the *E. coli* six-line 190 and 285 GHz spectra were nearly

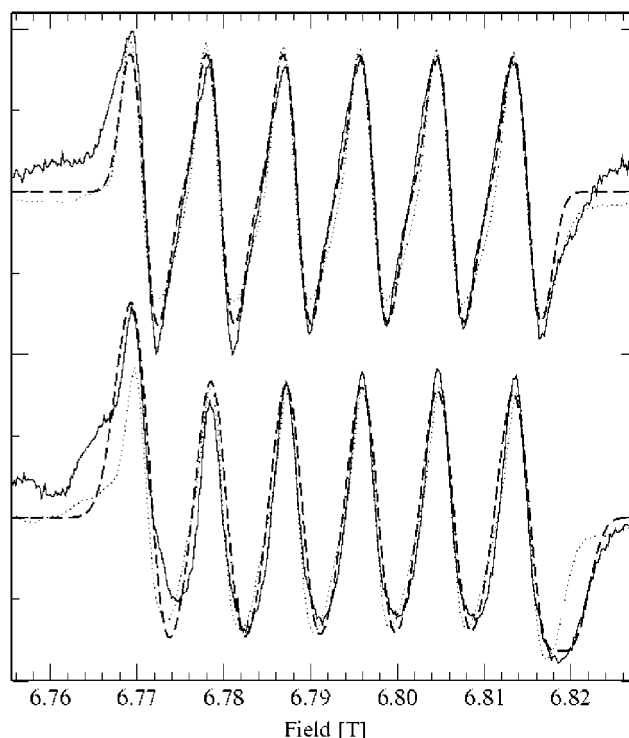


Figure 2. The 190 GHz EPR spectrum of the azide-complexed manganese SOD from *R. capsulatus* (lower) and *E. coli* (upper). Best-fit simulations are shown as dashed lines, and the corresponding field-shifted experimental 285 GHz spectra, also shown in Figure 1, are plotted as dotted lines. Best-fit magnetic parameters are given in Table 1. Spectra were obtained at 25 K with 20 G modulation under nonsaturating conditions.

identical. For the *R. capsulatus* protein, each of the 190 GHz hyperfine lines were broader than at 285 GHz and noticeably more asymmetric with the biggest effect on the highest-fieldline. The results of 190 GHz simulations using the same Hamiltonian used for the untreated samples are summarized in Figure 2 and Table 1. The *R. capsulatus* zero-field parameters were larger than those of the *E. coli* protein. This is consistent with the observation that the hyperfine line-width of the former is larger. These results suggest that the azide-complexed *R. capsulatus* Mn(II) center exists in a more asymmetric site than in the *E. coli* protein.

The structure of the *R. capsulatus* protein has not yet been solved. The high structural homology of all SODs suggests that the *R. capsulatus* protein will also be quite similar. By contrast, the HFEP results show that the protein–metal ion interactions are measurably different in the two manganese-containing SODs. Accurate measurements of the magnetic parameters using HFEP will now make it possible to examine the relationship between the magnetic state of the Mn(II) center and enzymatic activity. These results show that HFEP is an extremely sensitive method for probing the electronic environment around manganese centers.

Acknowledgment. We are grateful to A.W. Rutherford for encouragement and support. This work was supported by grants from the Human Frontier Science Organization (Contract RG0249) and the Région Ile-de-France (Contract Sésame) and Grant BID 1201/OC-AR, PICT 01-05105 from ANPCyT (N.C.).

Supporting Information Available: Spectrum of free Mn(II) in buffer compared to MnSOD at 190 GHz (PDF). This material is available free of charge via the Internet at <http://pubs.acs.org>.

JA016258M

(10) Uncertainties in the magnetic parameters of the native MnSODs were estimated by determining the change required for a given parameter to increase the root-mean-square difference between simulation and experimental spectrum by 10%. The errors were $\pm 20 \times 10^{-4} \text{ cm}^{-1}$ for the zero-field parameters, $\pm 6 \times 10^{-4} \text{ cm}^{-1}$ for the hyperfine coupling and ± 0.0001 for the *g*-value.

(11) Newman, D. J.; Urban, W. *Adv. Phys.* **1975**, *24*, 793–844. Heming, M.; Remme, S.; Lehmann, G. *J. Magn. Reson.* **1986**, *69*, 134–143.

(12) Griffith, J. S. *The Theory of Transition-Metal Ions*; University Press: Cambridge, 1964.

(13) Campbell, K. A.; Yikilmaz, E.; Grant, C. V.; Gregor, W.; Müller, A.-F.; Britt, R. D. *J. Am. Chem. Soc.* **1999**, *121*, 4714–4715.

(14) Whittaker, M. M.; Whittaker, J. W. *Biochemistry* **1996**, *35*, 6762–6770.